MRS Communications (2016), 6, 330–340
© Materials Research Society, 2016
doi:10.1557/mrc.2016.39

MRS Communications

Functional Oxides Prospective Article

Domain structures and magnetoelectric effects in multiferroic nanostructures

Deyang Chen, and **Xingsen Gao,** Guangdong Provincial Key Laboratory of Quantum Engineering and Quantum Materials, Institute for Advanced Materials, South China Normal University, Guangzhou 510006, China
Jun-Ming Liu, Laboratory of Solid State Microstructures, Innovation Center of Advanced Microstructures, Nanjing University, Nanjing 210093, China
Address all correspondence to Xingsen Gao, Jun-Ming Liu at **xingsengao@scnu.edu.cn**; **liujm@nju.edu.cn**

(Received 31 May 2016; accepted 29 August 2016)

Abstract

Multiferroic nanostructures have been attracting tremendous attention not only for novel phenomena associated with fundamental physics, but also due to exciting application potentials in future nanoelectronic devices. In this mini-review, we first introduce several fabrication techniques recently developed for single phase and composite multiferroic nanostructures. Then, the topologic vortex domain structures in various ferroic nanostructures, which may bring about additional fundamental discoveries and applications in ultrahigh density recording, are discussed. Particular attention is paid to magnetoelectric effects in multiferroic nanodots, including room temperature electric field induced magnetic domain switching. Finally, existing challenges and new directions, e.g., cross-couplings among multiple functionalities, are prospected. We genuinely hope that this mini-review will arouse the readers' interest in this fascinating field.

Introduction

Since 2003, the renaissance of multiferroics has been stimulated by several seminal works, including the discoveries of magnetoelectric (ME) responses in single-phase multiferroic $BiFeO_3$ (BFO) thin films,[1] magnetism-induced ferroelectricity in multiferroic manganites such as $TbMnO_3$,[2] and strong ME coupling in $CoFe_2O_4$ (CFO)/$BaTiO_3$ (BTO) multiferroic heterostructures,[3] unexpectedly igniting the tremendous flurry of interests in this field. The multiferroic nanostructures are of particular significance due to the high demand of the current miniaturization and multifunctional technological trends in microelectronic industry. In addition, the strong coupling between charge and spin degrees of freedom, i.e., the ME coupling in multiferroic nanostructures, allows for controlling magnetic order by electric field and vice versa.[4–7] Over the last decade, this field has been expanding rapidly, and a number of novel phenomena and promising application opportunities have been reported.[8–12]

Nowadays, device scale-down is being accelerated with the demands of high-performance and high-density data storage, while emergent physical phenomena can be expected when the materials are scaled down to nanoscale. Along this line, much attention has been attracted to developing new fabrication processes for high-density and high-quality multiferroic nanostructures, either single-phase materials or ferromagnetic/ferroelectric composites.[13,14] In ferroic nanodots, in contrast to the popular experimental works on ferromagnetic flux closure vortex domains,[15–17] the ferroelectric vortex domain structures remain experimentally elusive although theoretical predictions have been available for a long time.[18] Hence, a robust and controllable ferroelectric vortex remains highly favorable for future ultrahigh density applications. Besides, improved ME coupling in multiferroic nanodots,[19,20] owing to the release of clamping effect from the substrates and proper manipulating of domain structures, paves a pathway to realize enhanced cross-controls of ferroelectricity and magnetism by magnetic and electric stimuli. In particular, this may provide opportunities for the room temperature reversible control of magnetism, which is of first priority for the next generation memory devices.[20,21] Finally, the cross-couplings among multiple functionalities such as strain, magnetism, polarization, and optical properties, have also drawn some research attentions, and further new findings and application potentials may be expected in this new exciting area.[22–25]

In this mini-review, we emphasize on the domain structures and electric field control of magnetism in several multiferroic nanostructures. We will first introduce the schemes of connectivity between multiferroic nanostructures (e.g., nanodot arrays) and fabrication techniques. Then, a special focus on the flux closure polar vortex domains in ferroelectric nanodots will be described. Afterwards, the room temperature electric field control of nanoscale magnetic domain switching in various nanostructures, particularly the out-of-plane heterostructures compatible with the standard integrated electronics, will be reviewed. In the final section, future directions will be prospected. We genuinely hope that this mini-review will draw the readers' attention to the persistent challenges and future key directions in multiferroic nanostructures.

https://doi.org/10.1557/mrc.2016.39 Published online by Cambridge University Press

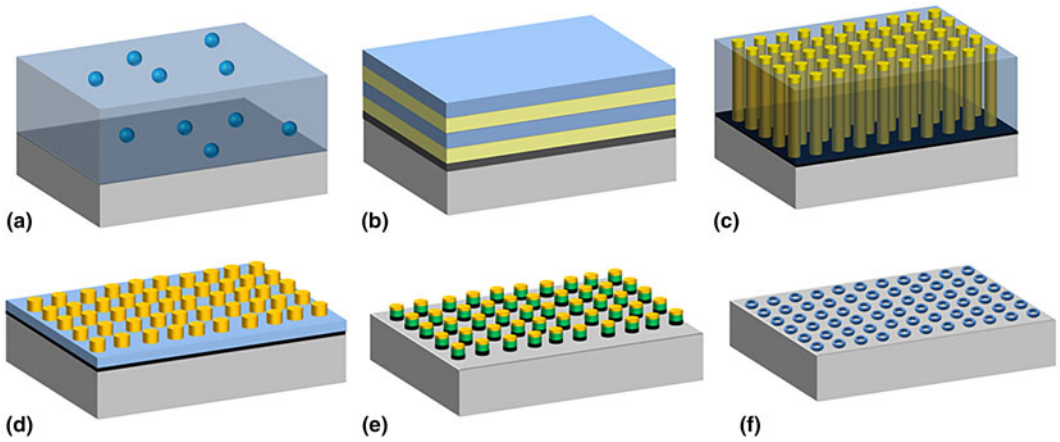


Figure 1. Schematics for different types of multiferroic nanostructures (a)–(f): (a) 0–3 type particulate nanocomposite films with magnetic particles embedded in the ferroelectric matrix, (b) 2–2 type layered heterostructures, (c) 1–3 type vertical heterostructures, (d) 0–2 type magnetic nanostructures on top of ferroelectric thin films, (e) 0–0 type layered heterostructured nanodot arrays, (f) multiferroic/ferroelectric/magnetic nanorings. The bottom layer (black color) in (b)–(e) is the bottom electrode, such as $SrRuO_3$, $La_{0.7}Sr_{0.3}MnO_3$, for studying the electric field control of magnetism in the multiferroic nanostructures.

Different types of multiferroic nanostructures

We first discuss several types of multiferroic composite nanostructures, which have been explored in the past decade, where the connectivity of the two and more components can greatly affect the ME properties. The most widely studied connectivity schemes include the 0–3 type particulate nanocomposite films, 2–2 type layered heterostructures, and 1–3 type vertical heterostructures,[26–30] as shown in Figs. 1(a)–1(c). In the 0–3 type composites, magnetic particles are randomly distributed in ferroelectric matrix, while a 2–2 type layered heterostructure usually consists of alternating layers (two layers, multilayers, or even superlattices) of ferroelectric components and magnetic ones. The 1–3 type vertical heterostructures are typically made of pillars of one material embedded in the matrix of another. Quite a few excellent reviews addressing these 0–3, 2–2, and 1–3 types multiferroic nanostructures are available. In particular, the 1–3 type nanostructures are appreciated because they exhibit large ME coupling effect due to the efficient release of clamping effects from the substrates.[11,31–33]

Recently, several 0–0 and 0–2 types of nanostructures, as displayed in Figs. 1(d) and 1(e), have been reported.[20,21,34,35] The 0–2 type multiferroic composites consist of ferroelectric films and magnetic nanostructures on top of them, allowing the electric field control of magnetic domain structures [Fig. 1(d)]. The less studied 0–0 type structures are mainly composed of ferroelectric–ferromagnetic epitaxial nanodot arrays [Fig. 1(e)] as well as recently reported multiferroic/ferroelectric/magnetic nanorings [Fig. 1(f)].[20,36] Compared with those structures mentioned earlier, the 0–0 type nanodots arrays demonstrate several apparent advantages.[19,20] First, they allow the atomic level mechanical coupling and concurrently avoid the substrate clamping in multiferroic composite films, benefiting to the ME coupling enhancement. The possibility for fabricating specific structures such as nanorings [Fig. 1(f)] and other multilayered geometries also enables us to explore additional geometric effects on domain structures and ME effects. Moreover, the 0–0 type multiferroic nanostructures are compatible with conventional semiconductor processing, with the ability to scale down to ultrahigh density and avoid the cross-talk effects among the neighboring dots. These advantages are highly preferred for applications in future multiferroic devices.

Fabrication of nanodot arrays

The fabrication of 0–3, 1–3, and 2–2 types of nanostructures have been addressed in previous review articles,[11,28,33] which is not our main focus. For high-density device applications and electric property characterizations of multiferroic nanostructures, the first priority is to fabricate high-quality epitaxial nano-island structures.[37,38] Along this line, several fabrication techniques developed in the past decade have been summarized by Han et al.,[13] such as the top-down approaches including the focused ion beam milling and electron beam direct writing, the bottom-up self-assembly method, and the modified bottom-up membrane mask or copolymer template-assisted deposition. The self-assembled method to produce the 1–3 type nanostructures has been reviewed by Liu et al.[32]

Furthermore, anodized alumina (AAO) template-assisted deposition method and the AAO template-assisted ion beam-etching technique have been attempted to produce high-quality epitaxial structures consisting of high-density 0–0 type ferroelectric/multiferroic nanodot arrays and nanorings.[20,39] Here, we highlight several examples including those accomplished in the authors' laboratory. Tian et al.[20] have just reported the fabrication of 0–0 type high-density and periodically ordered epitaxial CFO/BFO nanodot arrays by the AAO template-assisted pulsed laser deposition. As shown in Fig. 2(a), the AAO template mask was first transferred

https://doi.org/10.1557/mrc.2016.39 Published online by Cambridge University Press

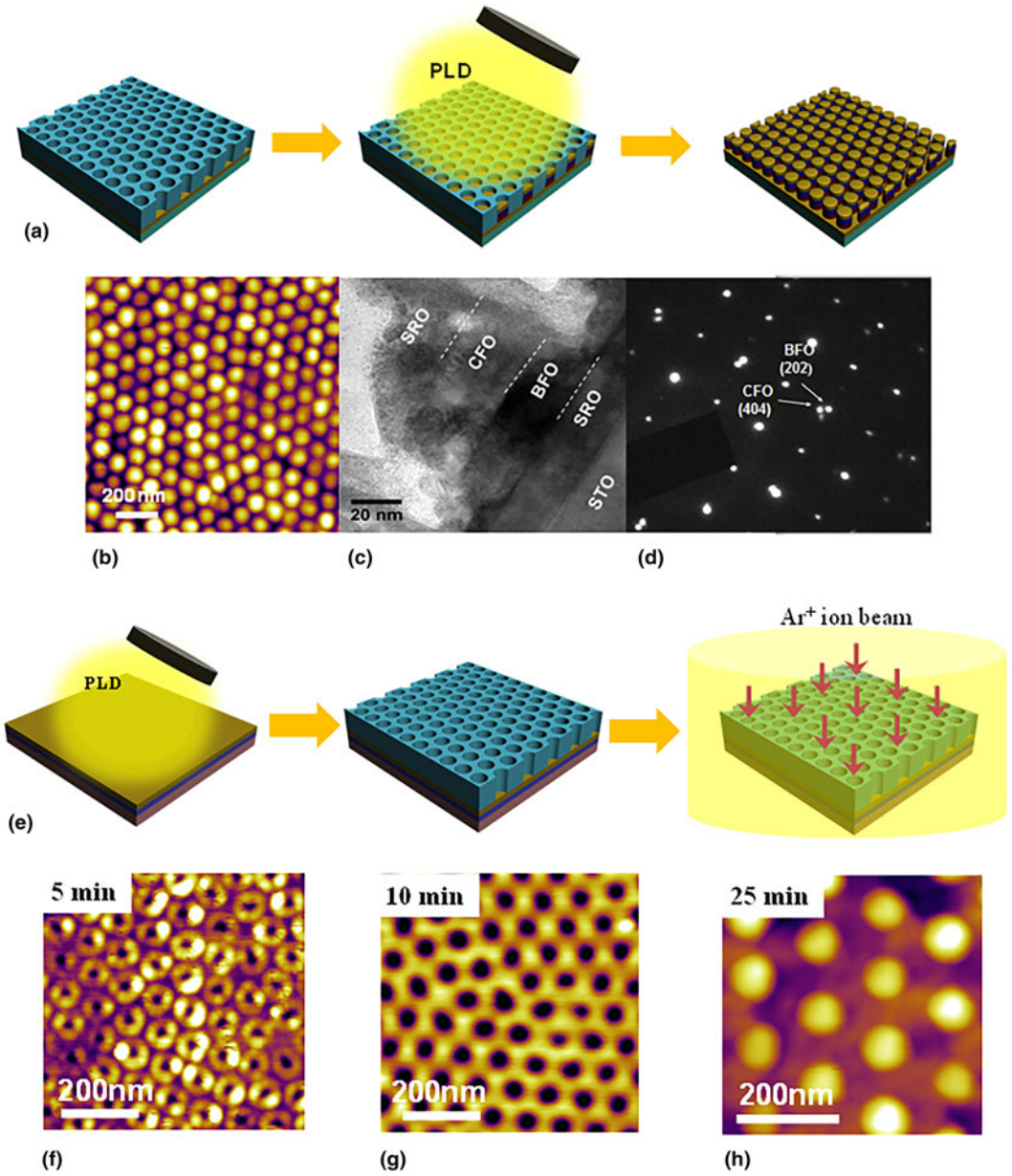


Figure 2. Fabrication of high-density epitaxial nanodot arrays by AAO template-assisted pulsed laser deposition (a)–(d): (a) Schematics of fabrication procedures, (b) AFM image of the obtained nanodot arrays, (c) cross-section TEM images of a BFO/CFO/SRO nanodot, (d) selected area electron diffraction pattern of the nanodots. Reproduced from Ref. 20 by permission of © 2016 American Chemical Society. Preparation of epitaxial nanoring like structure, anti-nanodot arrays, and nanodot arrays by AAO template-assisted ion beam etching method are demonstrated in (e)–(h):[39] (e) Schematic diagram for the AAO template-assisted ion beam-etching method. Panels (f)–(h) show the AFM images for the corresponding BFO nanostructure arrays produced after different etching durations from 5 to 25 min: (f) nanorings, (g) anti-nanodot arrays, and (h) nanodot arrays.

onto the $SrRuO_3$ (SRO) buffered $SrTiO_3$ (STO) substrate, and then the CFO/BFO nanodot arrays were sequentially prepared by pulsed laser deposition through the AAO template. Afterwards, the AAO mask was removed by mechanical or chemical lift-off to leave the nanodot arrays alone. The obtained nanodots exhibit an average lateral size of ~70 nm and neighboring dot–dot distance of ~110 nm [Fig. 2(b)]. The cross-section transmission electron microscopy (TEM) and selected-area electron diffraction confirmed the high quality and epitaxy of the BFO/CFO nanodot arrays [Figs. 2(c) and 2(d)]. In another work, Lu et al.[19] studied the similar 0–0 type BTO/CFO heterostructured nanostructures, which also exhibit some extent of ME coupling. This method enables a large-area fabrication of high-density well-ordered epitaxial nanodots, with the capability of scaling down to ~30 nm in diameter, yielding a pixel density higher than 100 Gbit/in.^{2}.

https://doi.org/10.1557/mrc.2016.39 Published online by Cambridge University Press

In addition, a novel route to fabricate the BFO nanodots and nanorings was proposed,[39] as illustrated in Fig. 2(e). Here, ion beam was used to etch the high-quality single-phase multiferroic BFO film through the AAO-template mask. By this approach, the BFO nanorings, nanodot arrays, and anti-nanodot arrays, can be fabricated by simply adjusting the etching duration, as shown in Figs. 2(f)–2(h). The step-by-step SEM study revealed the morphology evolution of the AAO mask layer from hole-array to dot-array during the etching process, and consequently the BFO film underneath the AAO template evolved into various nanostructured arrays. This method can also be extended to pattern a wide range of multiferroic/ferroelectric/magnetic nanostructures with adjustable shape, size, and pixel density, and it is thus promising in terms of fundamental research and for applications in high-density devices such as ultra-high-density recording devices.

Topological flux closure vortex domain structures

Domain structures are rather essential for ferroic materials, which not only greatly affect the ferroic functionalities such as piezoelectricity, electrical conductivity, magnetic exchange bias, but also largely determine the coupling between the inter-ferroic orders in multiferroic materials. It is suggested that the domain structures are critically dependent of the interplay among various energies such as exchange, electroelastic, and electrostatic energies with adjacent surface. All these ingredients of physics are however highly dimensionality-relevant.[40] Consequently, dimension reduction in ferroic nanostructures becomes an effective tool to manipulate the domain structures. Ferroic nanodot represents a typical geometry to illustrate such manipulation. In this section, we will pay attention to the nanoscale domain structures in ferroic nanodots, including several types of multiferroic nanodots.

Earlier investigations did explore several unique domain structures in ferroic nanostructures, such as single domain dots, bubble domains, and one-dimensional (1D) topological defects such as vortex, center types, and skyrmion domain structure, depending on different kinds of materials and geometries.[15,40,41] One of the most interesting systems is the flux closure vortex topological structures, which exist in nature over a wide range of scales, from galaxies and weather systems down to the flowers, as illustrated in Fig. 3(a). These exotic vortex topological defects in multiferroic/ferroelectric/magnetic materials are also attracting intensive attentions. Landau and Lifschitz[42] and Kittel[43] first predicted that the flux closure vortex domain structures possibly occur in ferromagnetic nanodots. Indeed, the vortex (skyrmion) structures in nanosized ferromagnets have been frequently reported due to their prominent demagnetization effect.[15,44] It was intensively studied for the purpose of high-density data storage. The skyrmion in ferromagnetic/multiferroic materials as a hot topic nowadays has also been observed in systems with large Dzyaloshinsky–Moriya (DM) effect.[45]

On the other hand, experimental observations of flux closure vortex domain in ferroelectrics are still elusive, although a number of theories predicted the existence of ferroelectric vortex.[18,49,50] Unlike the well-known skyrmion in nanosized ferromagnets, the flux closure vortex domains in ferroelectrics suffer from large electroelastic energy. Nevertheless, size reduction can help releasing such large electroelastic energy. In 2004, Naumov et al.[18] predicted that bi-stable polar vortex as small as 3.2 nm can be stable in highly depolarized ferroelectric nanodots [Figs. 3(b) and 3(c)], promising for ultrahigh storage density of 60 Tbit/in.^{2}, two orders of magnitude higher than conventional nonvolatile memories. In the meantime, since the interaction between vortex domains in different dots is generally weak, the problem of cross-talking between different memory units can thus be largely avoided. These advantages aroused a surge of research interests, and tremendous efforts have been placed on seeking ferroelectric vortex domains in various nanodots. Experimental evidences with the flux-closure domain structures have not been unveiled until recently, thanks to the emergence of powerful piezoresponse force microscopy (PFM) and advanced TEM technique.[40,46,47,51,52] Nelson et al.[53] and Jia et al.[54] identified half of a closure quadrant at the junction between ferroelectric domain walls and an interface in thin films of BFO and $PbTiO_3$ (PTO), respectively. The full closure quadrant was found by Gruverman et al.,[47] McGilly et al.,[55] and McQuaid et al.[56] in ferroelectric $BaTiO_3$ nanodots [Fig. 3(d)]. Rodriguez et al.[51] revealed the vortex polarization states in $Pb(Zr,Ti)O_3$ (PZT) nanodots using PFM assisted with theoretical predictions [Fig. 3(e)]. However, flux closure polarization vortex was not yet demonstratively observed in spite of available indirect evidence with their transient forms during the switching process,[47] until direct observations of the flux-closure domains and polar vortex in PTO/STO multilayers[57] and their superlattices [Fig. 3(f)],[48] respectively. The vortex domains are promising towards future nanoelectronics applications since their low dimensionality and specific momenta. These works pave the way to utilize the geometric parameters of ferroic nanostructures to tailor their domain structures and other related novel properties such as ME coupling, and the relevant techniques appear to be competitive for domain engineering and domain electronics.

Electric field control of magnetism

Electric field control of magnetism in multiferroics, aiming at new types of ultra-low-power consuming and high-density memories/logic devices, has been the focus of intensive researches.[7,58,59] In the multiferroic composites, electric field control of magnetism can be realized by means of either strain-mediated ME coupling across the interface, exchange coupling, or charge-driven ME coupling.[11,28,31,33] In another word, the ME effects can be obtained by the coupling between interfacing ferroelectric and ferromagnetic domains, leading to magnetic domain switching indirectly driven by ferroelectric domain switching triggered by electric field. Currently, the key

https://doi.org/10.1557/mrc.2016.39 Published online by Cambridge University Press

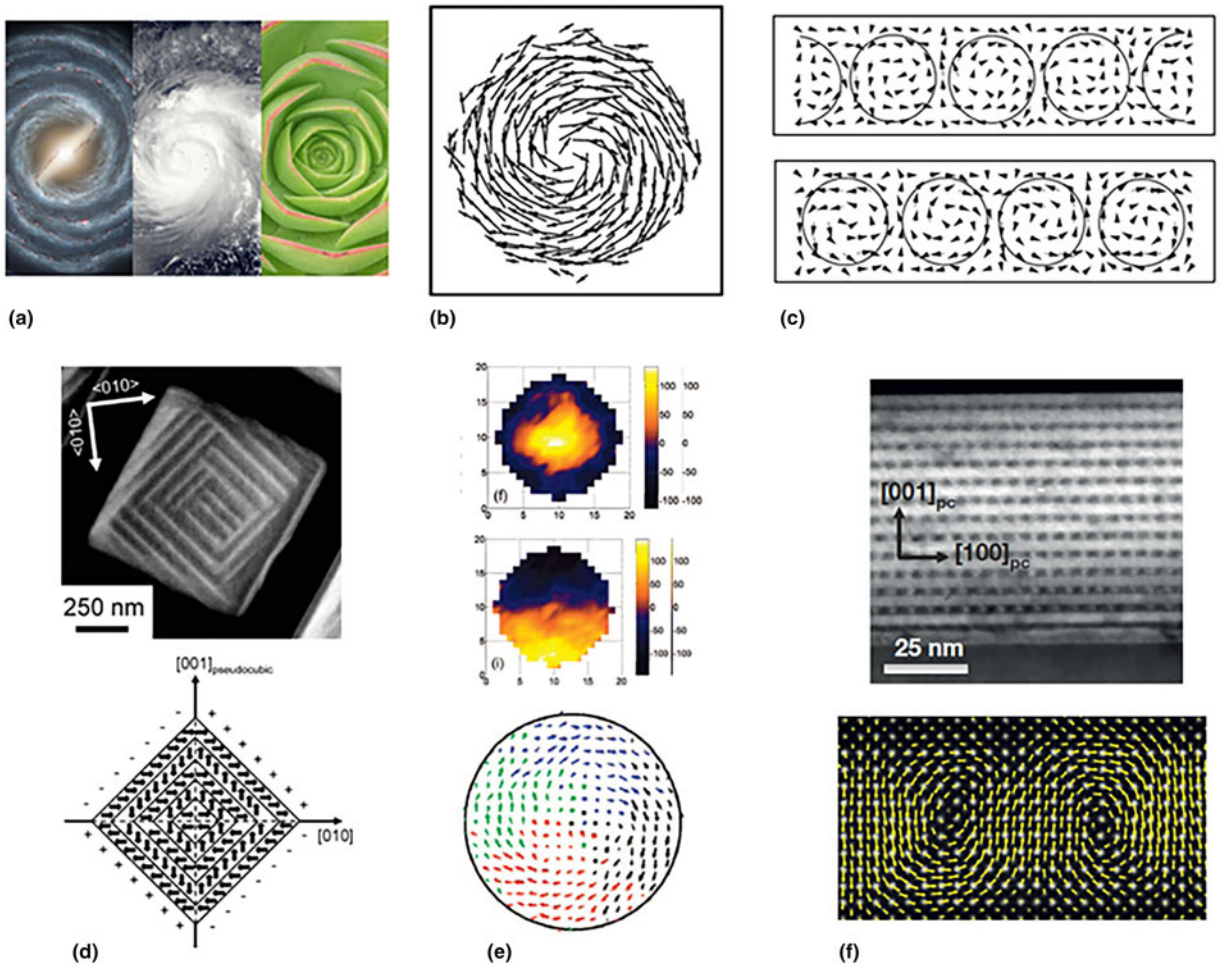


Figure 3. (a) Flux closure vortex structures in nature: galaxies system, weather system, and a flower. (b) A vortex in a ferroelectric nanodot along the central *z*-plane, and (c) arrays of vortices appear in the central *x* (as well as y) cross-section, theoretically predicted by Naumov et al. Reproduced from Ref. 18 by permission of © 2004 Nature Publishing Group. (d) Ferroelectric domains within the quadrants in $BaTiO_3$ nanodots, observed by TEM. Reproduced from Ref. 46 by permission of © 2009 American Chemical Society. (e) Vortex polarization states in PZT nanodots. Reproduced from Ref. 47 by permission of © 2009 American Chemical Society. (f) Flux closure vortex–antivortex arrays in PTO/STO superlattices, obtained by HRTEM. Reproduced from Ref. 48 by permission of © 2016 Nature Publishing Group.

challenge for the electrical control of magnetism is to achieve robust and reversible 180° switching of magnetization by electric field at room temperature. Nanoscale multiferroic nanostructures favor the domain structure manipulation, substrate clamping release, and domain stability alternation, while all of these mechanisms are effective roadmaps to achieve this goal.

We highlight several instances along this line. For a 0–2 type multiferroic system consisting of nickel nanomagnet on piezoelectric $Pb(Mg_{1/3}Nb_{2/3})O_3$–$PbTiO_3$ (PMN–PT) single-crystal substrate, the elastic coupling stems from the piezoelectric/magnetostrictive coupling via the interface, in which the ME coupling is indirect. It is rather difficult to realize the 180° switching of magnetic domains in such structure due to the twofold degeneracy of magnetization. However, if one takes advantage of the shape anisotropy by designing a specific geometric structure, the 180° domain switching can be obtained by applying two consequent electric pulses, as shown in Fig. 4. In the first negative electric pulse, the piezoelectric substrate PMN–PT generates a compressive strain on the nanomagnet, which provides an extra anisotropy with the easy axis along the *x*-axis to rotate the magnetic orientation for 90°. The second positive electric pulse generates an easy axis along the *y*-axis, leading to another 90° rotation; thus a 180° reverse can be achieved.[60] This indicates that it is possible to achieve the 180° domain switching of nanomagnets by properly adjusting the shape anisotropy and interface coupling.

Electric field control of nanoscale magnetic domain through the exchange coupling between antiferromagnetic BFO and magnetic nanostructures was also explored. In 2006, Zhao et al.[61] demonstrated the room temperature electric field control of antiferromagnetic order in multiferroic BFO films. Later, Chu et al.[62] successfully reversibly rotated the in-plane

https://doi.org/10.1557/mrc.2016.39 Published online by Cambridge University Press

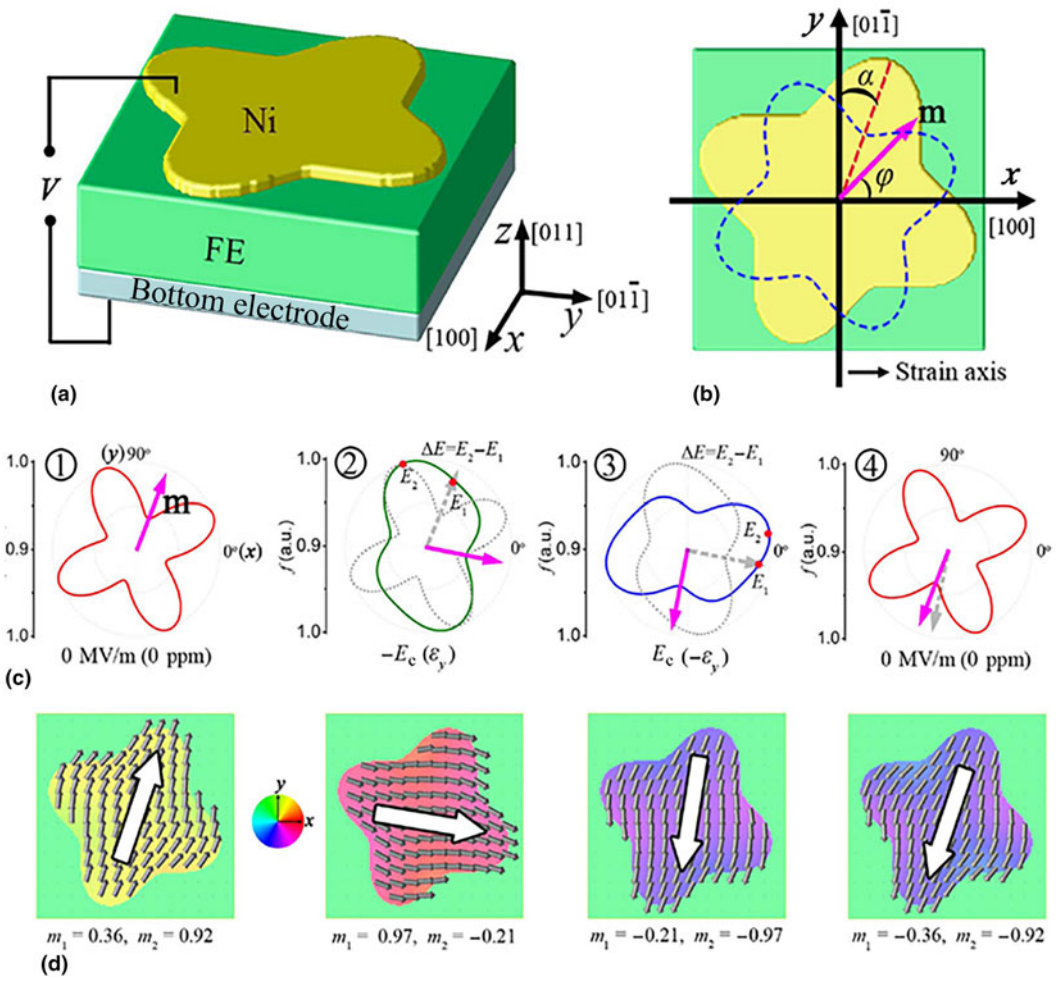


Figure 4. Morphologically engineered artificial multiferroic heterostructure. (a) Schematic of the heterostructure of a patterned nanomagnet with fourfold shape symmetry grown on a ferroelectric layer [e.g., (011)-PMN–PT]. (b) The top view of the Ni nanomagnet on the ferroelectric layer, where *y*-axis denotes the main direction of in-plane anisotropic piezostrain and the angle between *y*-axis and one of the long axes of the Ni nanomagnet. The blue dashed line represents the shape anisotropy energy contour at initial states. Mechanisms of the 180° reversal: (c) Energy polar diagrams of the Ni nanomagnet upon the application of zero electric field (as-grown state), and then successive fields of $-E_c$, E_c, and zero. Here the gray-dashed and magenta-solid arrows represent the previous and present states of *m*, respectively, and the energy barrier $\Delta E = E_2 - E_1$ ensures the magnetization switch unidirectionally from ① state to ② state, and from ③ state to ④ state, respectively. (d) Magnetization vector diagrams corresponding to (c), in which the different background colors represent the orientations of the magnetization as indicated by the color wheel. Reproduced from Ref. 60 by permission of © 2014 Nature Publishing Group.

magnetic domain of $Co_{0.9}Fe_{0.1}$ (CoFe) nanomagnets for 90° at room temperature by electric field, using the exchange coupling-mediated ME effect in the CoFe/BFO system, a 0–2 type structure. In the latter study, a room temperature in-plane electric field induced 180° magnetization reversal was achieved, through the in-plane switching of stripe-like 71° ferroelectric domain pattern.[63] From a device point of view, it is more important to achieve an out-of-plane electric field control of magnetism, which is more compatible with current microelectronic device process. Recently, Heron et al.[21] reported a seminal work on the out-of-plane electric field deterministic control of magnetism at room temperature in the CoFe/BFO spin valve device, using the exchange-mediated ME effects [Fig. 5(a)]. To probe the domain structures and the net magnetic moment, the x-ray magnetic circular dichroism photoemission electron microscopy (XMCD-PEEM) images of the Pt/CoFe/BFO system were taken in the initial state and after application of 6 V, where the incident x-ray was aligned perpendicular and parallel to the stripe like 71° domains [Fig. 5(b)], respectively. It turns out that the net CoFe magnetization can be reversed by applying an electric field as low as 6 V [Fig. 5(c)], thanks to the coupling between the magnetic DM vector and ferroelectric polarization in the BFO layer. However, the reliability issue for such reversible switching is still a great challenge for the actual device applications, as it is still difficult to obtain more than three switching cycles in the current devices.

In addition, the out-of-plane electric field control of magnetic domain switching in 0–0 type multiferroic structures is also

https://doi.org/10.1557/mrc.2016.39 Published online by Cambridge University Press

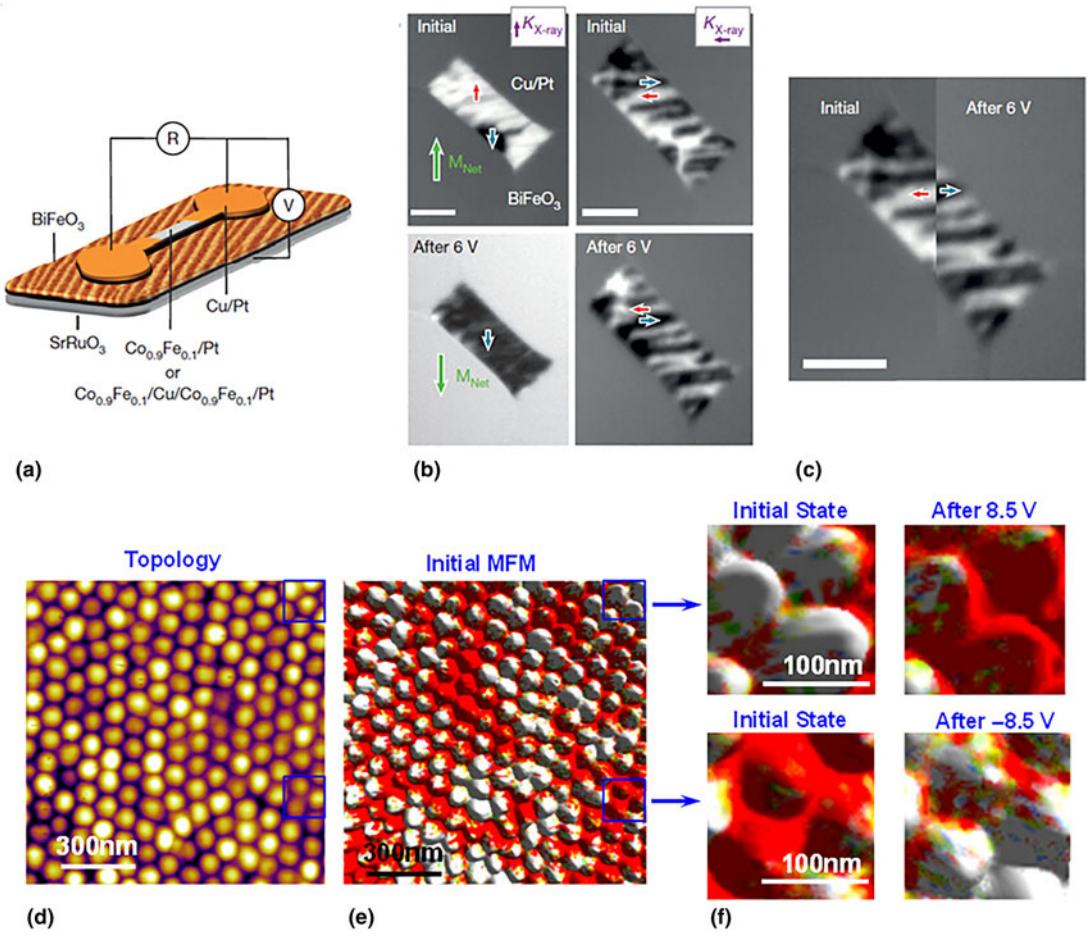


Figure 5. Electric field control of magnetism in a 0–2 type multiferroic nanostructure (a)–(c): (a) Schematic of a ME device consisting of either CoFe or a $Co_{0.9}Fe_{0.1}$/Cu/CoFe spin valve on $BiFeO_3$. (b) Initial and final (after 6 V) directions of the in-plane CoFe moments imaged with a vertical $K_{X\text{-}ray}$ and horizontal $K_{X\text{-}ray}$ XMCD-PEEM. (c) The domain pattern switches and net CoFe magnetization reverses after the voltage is applied. Scale bars are 2 μm in (b) and (c). Reproduced from Ref. 21 by permission of © 2014 Nature Publishing Group. Electric field control of magnetization in 0–0 type multiferroic nanostructured nanodot arrays (d)–(f): (d) AFM topology image, (e) MFM micrograph superimposed with its corresponding 3D topographic image. (f) The selected area magnified MFM images superimposed with their 3D topologies before and after applying electric field of ±8.5 V bias voltages. Reproduced from Ref. 20 by permission of © 2016 American Chemical Society.

highly desired. Recently, the 0–0 type CFO/BFO heterostructured nanodots have been developed by Tian et al.,[20] and the electric field control of magnetization reversal based on a combination of strain-mediated and exchange-mediated ME effects was also demonstrated, as shown in Figs. 5(d)–5(f). To display the domain structure evolution in the nanodot arrays, the magnetic force microscopy (MFM) images were superimposed onto the corresponding 3D surface topology images, as shown in Fig. 5(e). An apparent variation of the MFM contrast occurred upon the electric field poling. For a clearer presentation, two small regions were pitched up to illustrate the domain switching in a bigger magnification. One sees clearly the magnetization switching of the nanodots to the opposite orientations, as reflected by the apparent contrast reversal shown in the MFM image [Fig. 5(f)]. Although such electric-field-induced magnetic switching is not well controllable, an opportunity for low-energy-consumption and high-density recording devices is open.

Outlook

Currently, exciting findings in nanostructured multiferroics have been obtained, which triggers interest in new mechanisms and methods to tailor the inter-ferroic couplings. In particular, novel aspects of electric field control of magnetic domain switching are highly appealed. However, there are still some further studies needed to achieve breakthroughs and to push this area to real applications.

Fabrication of high-density arrays

With the continued demand for ultra-high-density data storage applications, it is becoming increasingly important to scale down the dimension of multiferroic structures to nanoscale arrays such as nanodot arrays. However, there is a great challenge to prepare high-quality nanodots with diameter below 30 nm using the traditional AAO template process, since this method

https://doi.org/10.1557/mrc.2016.39 Published online by Cambridge University Press

requires very stringent deposition parameters that are unfavorable, and smaller pore mouth would be more easily blocked during the deposition of multiferroic materials. Polystyrene spheres template with ion beam-etching method could be another alternative. Our unpublished research shows that this method can be a facile route to fabricate high-quality multiferroic nanodot arrays with excellent epitaxial structure and multiferroic properties close to their parent films. Small copolymer templates could also be used to obtain nanodots as small as ~20 nm; however, their overall quality and order arrangement need to be further improved.

Domain design and manipulation

Although some indications of flux closure vortex-like behaviors are available, there is still no direct evidence with the ferroelectric flux closure vortex in isolated multiferroic/ferroelectric nanodots, while well-established vortex in PTO/STO superlattices was reported.[48] The difficulty lies in that a simple quadrant arrangement generates enormous disclination strain, which prevents the formation of vortex. If the size of nanodot is smaller than the critical point, alleviation of associated stresses will allow the depolarization effect to turn the polarization into flux closure vortex domain. Thus, sufficiently small size and high depolarization field are required to achieve the vortex domain, as supported by the observation of vortex arrays in PTO/STO superlattices, which is well consistent with the prediction by Naumov et al.[18] In addition, multiferroic/ferroelectric nanorings may help to stable the vortex configuration due to the absence of highly energetic vortex core. Moreover, whether the vortex structure can be manipulated by external stimuli, e.g., a robust and electric field well-controllable vortex domain, is still the target of further efforts. Furthermore, other ferroelectric topologic domain structures such as skyrmions and center domain also need further explorations, which may lead to new discoveries as well as application potentials.

Besides, geometric effect in nanodots is an effective tool to manipulate both ferroelectric and magnetic domain structures as well, which provides a new method to tailor the ME effects. Previous work demonstrated that it is possible to achieve electric field induced 180° magnetic switching.[21] Further work is still needed to obtain reversible switching in high-density nanodot arrays to pave the way for devices applications.

Room temperature electric field control of exchange bias

In the ferromagnet/BFO heterostructures, the exchange bias arising from the BFO domain walls and ME coupling between the ferromagnetic layer and antiferromagnetic BFO layer offer another possibility to achieve room temperature electric field control of exchange bias. Reversible electric field control of exchange bias has been achieved in a $LaSr_{0.7}Mn_{0.3}O_3/BiFeO_3$ (LSMO/BFO) field effect device structures, however, it has to be done below 10 K.[64,65] Martin et al.[66,67] have demonstrated a very large room temperature exchange bias (150–200 Oe) in the CoFe/BFO system, but electric field control of exchange bias has not yet been demonstrated. Recently, Allibe et al.[68] reported that the exchange bias can be electrically manipulated in a CoFeB/BFO-based spin valve, revealed by giant magnetoresistance (GMR) measurement (Fig. 6). Nevertheless, the switching is not very reversible, and they failed to restore any exchange bias in the subsequent cycles by applying the opposite voltage or by other voltage protocols. One possible reason is that the exchange bias arises from the pinned uncompensated spins at 109° domain walls of BFO, while the 109° domains are gradually switched to 71° domains or mono-domains (which has no pinned uncompensated spins) upon further polarization reverse cycles, resulting in the decline of exchange bias.[67,69] Therefore, stable and reversible electric field switching of 109° domains is crucial for achieving room temperature reversible electric field control of exchange bias. Specific techniques, such as using multiferroic BFO nanodots, which will reduce the

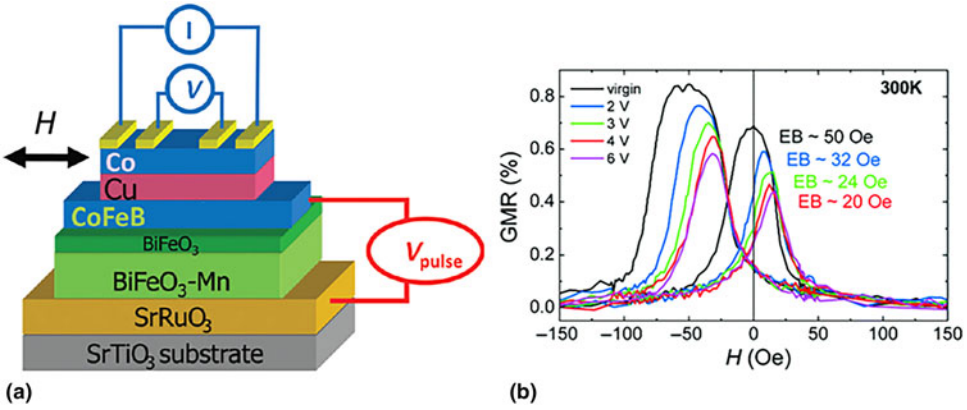


Figure 6. (a) Schematic of the spin valve device. (b) GMR curves of the spin valve after different electric pulses applied. Reproduced from Ref. 68 by permission of © 2012 American Chemical Society.

https://doi.org/10.1557/mrc.2016.39 Published online by Cambridge University Press

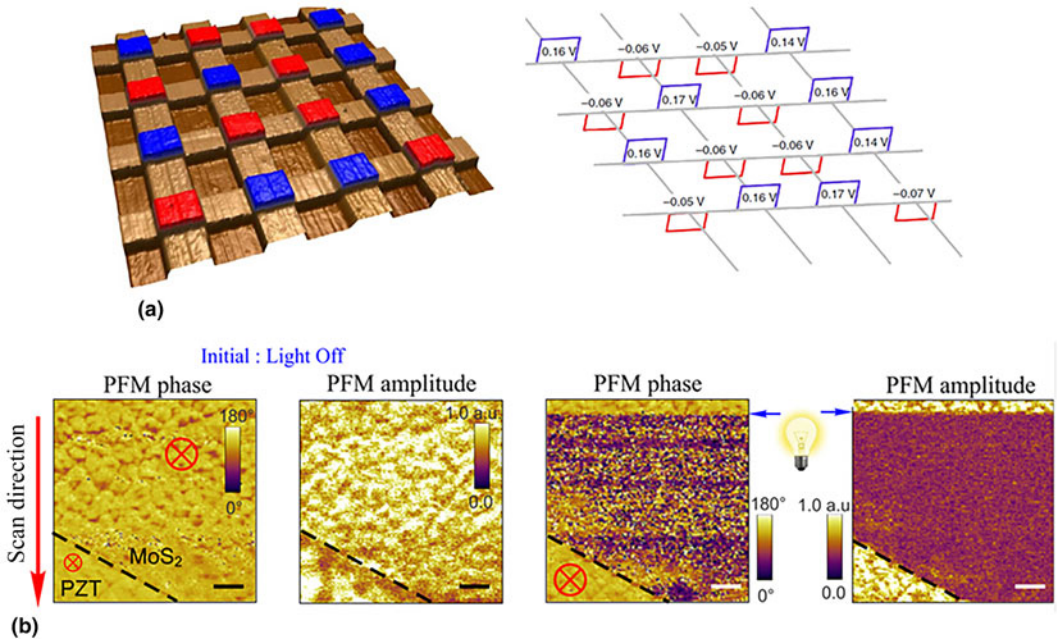


Figure 7. (a) A prototype of a 16-cell ferroelectric photovoltaic memory based on the cross-bar architecture, in which the photovoltaic voltages can be switched by the polarization reversal. Reproduced from Ref. 22 by permission of © 2013 Nature Publishing Group. (b) Optical light induced polarization switching in PZT with MoS_2 top electrodes, in which one can see the apparent contrast change in both PFM phase and amplitude after illumination of optical light. Reproduced from Ref. 24 by permission of © 2015 American Chemical Society.

clamping effect from the substrate, may help to solve this problem.

Cross-couplings between strain, ferroelectricity, magnetism, and optical properties

In literature on multiferroics, ME coupling is the main focus, while some more couplings may occur among strain, ferroelectricity, magnetism, and optical properties, which may give rise to multifunctional cross-couplings. For instance, a ferroelectric photovoltaic prototype 16-cell memory shown in Fig. 7(a) reveals the coupling between ferroelectricity and photovoltaic properties, allowing the polarization modulation of photovoltaic properties.[22] And optical light-induced ferroelectric switching was also reported in PZT films with molybdenum disulfide (MoS_2) transparent top electrodes by Gruverman's

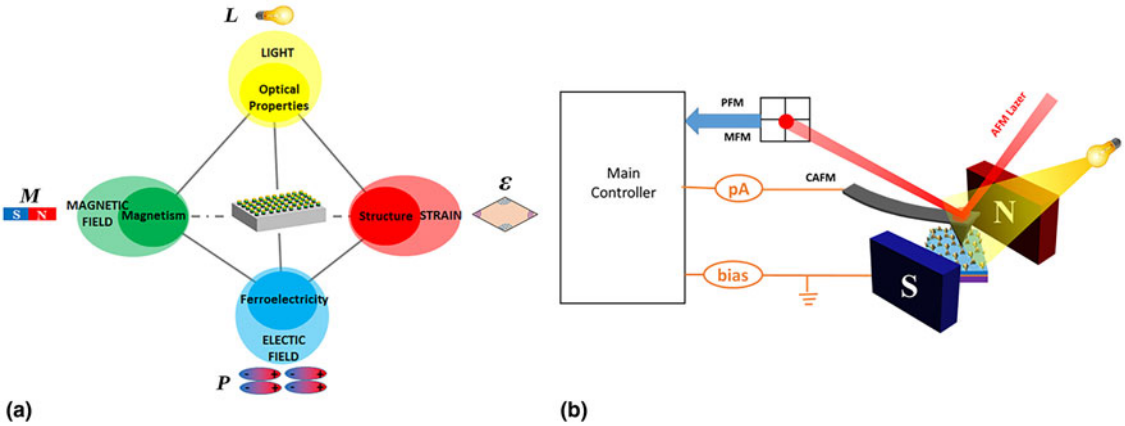


Figure 8. (a) Sketch of possible couplings between the various functionalities. (b) A proposed multifunctional SPM system for characterization of multifunctional couplings, which enables in situ measurements of PFM, MFM, C-AFM, and near-field optical properties, under various electric field, magnetic field, optical light, heat, and environmental conditions.

https://doi.org/10.1557/mrc.2016.39 Published online by Cambridge University Press

group [see Fig. 7(b)].[24] Chu and co-workers demonstrated the phenomenon of magnetic switching triggered by an ultrafast layer beam in CFO/SRO (1–3) type columnar composite, through the photorestriction from SRO layer.[23] The ferroelectric control of field-effect transistors enhanced using monolayer black phosphorus as the interfacial layer was predicted.[70] The coexistence of remarkable structural, ferroelectric, magnetic, and optical properties, as well the cross-couplings among them [see Fig. 8(a)], with the inputs of strain, electric field, magnetic field, and light, endows multiferroic nanostructures with a unique potential for multifunctional devices in electronics, spintronics, piezotronics, photonics, etc. providing a fantastic playground to engineer novel physical properties. To explore the nanoscale cross-couplings in low-dimensional nanostructures, new nanoscale multi-physic properties testing and tailoring systems are very indispensable, such as a multifunctional scanning probe microscopy (SPM) system [Fig. 8 (b)], which enables in-situ measurements of PFM, MFM, conductive atomic force microscopy (C-AFM), and near-field optical properties, under various electric field, magnetic field, optical light, heat, and environmental conditions.

Acknowledgments

The authors would like to thank the Natural Science Foundation of China (Grant No. 51272078, 51431006), the Project for Guangdong Province Universities and Colleges Pearl River Scholar Funded Scheme (2014), Science and Technology Planning Project of Guangdong Province (Grant No. 2015B090927006), the Natural Science Foundation of Guangdong Province (Grant No. 2016A030308019), and the International Science & Technology Cooperation Platform Program of Guangzhou (Grant No. 2014J4500016).

References

1. J. Wang, J.B. Neaton, H. Zheng, V. Nagarajan, S.B. Ogale, B. Liu, D. Viehland, V. Vaithyanathan, D.G. Schlom, U.V. Waghmare, N. A. Spaldin, K.M. Rabe, M. Wuttig, and R. Ramesh: Epitaxial $BiFeO_3$ multiferroic thin film heterostructures. *Science* **299**, 1719 (2003).
2. T. Kimura, T. Goto, H. Shintani, K. Ishizaka, T. Arima, and Y. Tokura: Magnetic control of ferroelectric polarization. *Nature* **426**, 55 (2003).
3. H. Zheng, J. Wang, S.E. Lofland, Z. Ma, L. Mohaddes-Ardabili, T. Zhao, L. Salamanca-Riba, S.R. Shinde, S.B. Ogale, F. Bai, D. Viehland, Y. Jia, D.G. Schlom, M. Wuttig, A. Roytburd, and R. Ramesh: Multiferroic $BaTiO_3$–$CoFe_2O_4$ nanostructures. *Science* **303**, 661 (2004).
4. Y. Tokura: Multiferroics-toward strong coupling between magnetization and polarization in a solid. *J. Magn. Magn. Mater.* **310**, 1145 (2007).
5. Y. Tokura and S. Seki: Multiferroics with spiral spin orders. *Adv. Mater.* **22**, 1554 (2010).
6. R. Ramesh and N.A. Spaldin: Multiferroics: progress and prospects in thin films. *Nat. Mater.* **6**, 21 (2007).
7. K.F. Wang, J.M. Liu, and Z.F. Ren: Multiferroicity: the coupling between magnetic and polarization orders. *Adv. Phys.* **58**, 321 (2009).
8. N.A. Spaldin and M. Fiebig: The renaissance of magnetoelectric multiferroics. *Science* **309**, 391 (2005).
9. S. Dong, J.-M. Liu, S.-W. Cheong, and Z. Ren: Multiferroic materials and magnetoelectric physics: symmetry, entanglement, excitation, and topology. *Adv. Phys.* **64**, 519 (2015).
10. N.A. Spaldin, S.-W. Cheong, and R. Ramesh: Multiferroics: past, present, and future. *Phys. Today* **63**, 38 (2010).
11. C.-W. Nan, M.I. Bichurin, S. Dong, D. Viehland, and G. Srinivasan: Multiferroic magnetoelectric composites: historical perspective, status, and future directions. *J. Appl. Phys.* **103**, 031101 (2008).
12. W. Ratcliff, J.W. Lynn, V. Kiryukhin, P. Jain, and M.R. Fitzsimmons: Magnetic structures and dynamics of multiferroic systems obtained with neutron scattering. *NPJ Quantum Mater.* **1**, 16003 (2016).
13. H. Han, Y. Kim, M. Alexe, D. Hesse, and W. Lee: Nanostructured ferroelectrics: fabrication and structure-property relations. *Adv. Mater.* **23**, 4599 (2011).
14. I. Jung and J.Y. Son: Dip-Pen Lithography of $BiFeO_3$ nanodots. *J. Am. Ceram. Soc.* **95**, 3716 (2012).
15. T. Shinjo, T. Okuno, R. Hassdorf, K. Shigeto, and T. Ono: Magnetic vortex core observation in circular dots of permalloy. *Science* **289**, 930 (2000).
16. B. Van Waeyenberge, A. Puzic, H. Stoll, K.W. Chou, T. Tyliszczak, R. Hertel, M. Fahnle, H. Bruckl, K. Rott, G. Reiss, I. Neudecker, D. Weiss, C.H. Back, and G. Schutz: Magnetic vortex core reversal by excitation with short bursts of an alternating field. *Nature* **444**, 461 (2006).
17. K. Yamada, S. Kasai, Y. Nakatani, K. Kobayashi, H. Kohno, A. Thiaville, and T. Ono: Electrical switching of the vortex core in a magnetic disk. *Nat. Mater.* **6**, 269 (2007).
18. I.I. Naumov, L. Bellaiche, and H. Fu: Unusual phase transitions in ferroelectric nanodisks and nanorods. *Nature* **432**, 737 (2004).
19. X. Lu, Y. Kim, S. Goetze, X. Li, S. Dong, P. Werner, M. Alexe, and D. Hesse: Magnetoelectric coupling in ordered arrays of multilayered heteroepitaxial $BaTiO_3/CoFe_2O_4$ nanodots. *Nano Lett.* **11**, 3202 (2011).
20. G. Tian, F.Y. Zhang, J.X. Yao, H. Fan, P.L. Li, Z.W. Li, X. Song, X.Y. Zhang, M.H. Qin, M. Zeng, Z. Zhang, J.J. Yao, X.S. Gao, and J.M. Liu: Magnetoelectric coupling in well-ordered epitaxial $BiFeO_3/CoFe_2O_4/SrRuO_3$ heterostructured nanodot array. *ACS Nano* **10**, 1025 (2016).
21. J.T. Heron, J.L. Bosse, Q. He, Y. Gao, M. Trassin, L. Ye, J.D. Clarkson, C. Wang, J. Liu, S. Salahuddin, D.C. Ralph, D.G. Schlom, J. Iniguez, B.D. Huey, and R. Ramesh: Deterministic switching of ferromagnetism at room temperature using an electric field. *Nature* **516**, 370 (2014).
22. R. Guo, L. You, Y. Zhou, Z. Shiuh Lim, X. Zou, L. Chen, R. Ramesh, and J. Wang: Non-volatile memory based on the ferroelectric photovoltaic effect. *Nat. Commun.* **4**, 1990 (2013).
23. H.J. Liu, L.Y. Chen, Q. He, C.W. Liang, Y.Z. Chen, Y.S. Chien, Y.H. Hsieh, S.J. Lin, E. Arenholz, C.W. Luo, Y.L. Chueh, Y.C. Chen, and Y.H. Chu: Epitaxial photostriction-magnetostriction coupled self-assembled nanostructures. *ACS Nano* **6**, 6952 (2012).
24. A. Lipatov, P. Sharma, A. Gruverman, and A. Sinitskii: Optoelectrical molybdenum disulfide (MoS_2)-ferroelectric memories. *ACS Nano* **9**, 8089 (2015).
25. R.O. Cherifi, V. Ivanovskaya, L.C. Phillips, A. Zobelli, I.C. Infante, E. Jacquet, V. Garcia, S. Fusil, P.R. Briddon, N. Guiblin, A. Mougin, A. A. Ünal, F. Kronast, S. Valencia, B. Dkhil, A. Barthélémy, and M. Bibes: Electric-field control of magnetic order above room temperature. *Nat. Mater.* **13**, 345 (2014).
26. J.H. Li, I. Levin, J. Slutsker, V. Provenzano, P.K. Schenck, R. Ramesh, J. Ouyang, and A.L. Roytburd: Self-assembled multiferroic nanostructures in the $CoFe_2O_4$–$PbTiO_3$ system. *Appl. Phys. Lett.* **87**, 072909 (2005).
27. F. Zavaliche, T. Zhao, H. Zheng, F. Straub, M.P. Cruz, P.L. Yang, D. Hao, and R. Ramesh: Electrically assisted magnetic recording in multiferroic nanostructures. *Nano Lett.* **7**, 1586 (2007).
28. Y. Wang, J.M. Hu, Y.H. Lin, and C.W. Nan: Multiferroic magnetoelectric composite nanostructures. *NPG Asia Mater.* **2**, 61 (2010).
29. Q. Miao, M. Zeng, Z. Zhang, X. Lu, J. Dai, X. Gao, and J.-M. Liu: Self-assembled nanoscale capacitor cells based on ultrathin $BiFeO_3$ films. *Appl. Phys. Lett.* **104**, 182903 (2014).
30. F.Y. Zhang, Q. Miao, G. Tian, Z.X. Lu, L.N. Zhao, H. Fan, X. Song, Z.W. Li, M. Zeng, X.S. Gao, and J.M. Liu: Unique nano-domain structures in self-assembled $BiFeO_3$ and $Pb(Zr,Ti)O_3$ ferroelectric nanocapacitors. *Nanotechnology* **27**, 015703 (2016).
31. J. Ma, J. Hu, Z. Li, and C.-W. Nan: Recent progress in multiferroic magnetoelectric composites: from bulk to thin films. *Adv. Mater.* **23**, 1062 (2011).
32. H.J. Liu, W.I. Liang, Y.H. Chu, H.M. Zheng, and R. Ramesh: Self-assembled vertical heteroepitaxial nanostructures: from growth to functionalities. *MRS Commun.* **4**, 31 (2014).

https://doi.org/10.1557/mrc.2016.39 Published online by Cambridge University Press

33. C.A.F. Vaz, J. Hoffman, C.H. Ahn, and R. Ramesh: Magnetoelectric coupling effects in multiferroic complex oxide composite structures. *Adv. Mater.* **22**, 2900 (2010).
34. L.N. Zhao, Z.X. Lu, F.Y. Zhang, G. Tian, X. Song, Z.W. Li, K.R. Huang, Z. Zhang, M.H. Qin, S.J. Wu, X.B. Lu, M. Zeng, X.S. Gao, J.Y. Dai, and J.M. Liu: Current rectifying and resistive switching in high density $BiFeO_3$ nanocapacitor arrays on Nb-$SrTiO_3$ substrates. *Sci. Rep.* **5**, 9680 (2015).
35. X.S. Gao, B.J. Rodriguez, L.F. Liu, B. Birajdar, D. Pantel, M. Ziese, M. Alexe, and D. Hesse: Microstructure and properties of well-ordered multiferroic $Pb(Zr,Ti)O_3/CoFe_2O_4$ nanocomposites. *ACS Nano* **4**, 1099 (2010).
36. K. Cho, G. Loget, and R.M. Corn: Lithographically patterned nanoscale electrodeposition of plasmonic, bimetallic, semiconductor, magnetic, and polymer nanoring arrays. *J. Phys. Chem. C* **118**, 28993 (2014).
37. J.F. Scott: Applications of modern ferroelectrics. *Science* **315**, 954 (2007).
38. N. Ortega, K. Ashok, J.F. Scott, and S.K. Ram: Multifunctional magnetoelectric materials for device applications. *J. Phys.—Condens. Mater.* **27**, 504002 (2015).
39. G. Tian, L. Zhao, Z. Lu, J. Yao, H. Fan, Z. Li, P. Li, D. Chen, X. Zhang, M. Qin, M. Zeng, Z. Zhang, J. Dai, X. Gao, and J.-M. Liu: Fabrication of periodically ordered $BiFeO_3$ nanostructured arrays by template-assisted ion beam etching method. *Under review.*
40. G. Catalan, J. Seidel, R. Ramesh, and J.F. Scott: Domain wall nanoelectronics. *Rev. Mod. Phys.* **84**, 119 (2012).
41. X.S. Gao, F. Xue, M.H. Qin, J.M. Liu, B.J. Rodriguez, L.F. Liu, M. Alexe, and D. Hesse: Bubble polarization domain patterns in periodically ordered epitaxial ferroelectric nanodot arrays. *J. Appl. Phys.* **110**, 052006 (2011).
42. L.D. Landau and E. Lifschitz: On the theory of the dispersion of magnetic permeability in ferromagnetic bodies. *Phys. J. Sowjetunion* **8**, 153 (1935).
43. C. Kittel: Theory of the dispersion of magnetic permeability in ferromagnetic materials at microwave frequencies. *Phys. Rev.* **70**, 281 (1946).
44. K.Y. Guslienko, X.F. Han, D.J. Keavney, R. Divan, and S.D. Bader: Magnetic vortex core dynamics in cylindrical ferromagnetic dots. *Phys. Rev. Lett.* **96**, 067205 (2006).
45. S. Seki, X.Z. Yu, S. Ishiwata, and Y. Tokura: Observation of skyrmions in a multiferroic material. *Science* **336**, 198 (2012).
46. A. Schilling, D. Byrne, G. Catalan, K.G. Webber, Y.A. Genenko, G.S. Wu, J.F. Scott, and J.M. Gregg: Domains in ferroelectric nanodots. *Nano Lett.* **9**, 3359 (2009).
47. A. Gruverman, D. Wu, H.J. Fan, I. Vrejoiu, M. Alexe, R.J. Harrison, and J.F. Scott: Vortex ferroelectric domains. *J. Phys.—Condens. Mater.* **20**, 342201 (2008).
48. A.K. Yadav, C.T. Nelson, S.L. Hsu, Z. Hong, J.D. Clarkson, C. M. Schlepuetz, A.R. Damodaran, P. Shafer, E. Arenholz, L.R. Dedon, D. Chen, A. Vishwanath, A.M. Minor, L.Q. Chen, J.F. Scott, L. W. Martin, and R. Ramesh: Observation of polar vortices in oxide superlattices. *Nature* **530**, 198 (2016).
49. I. Naumov and H. Fu: Vortex-to-polarization phase transformation path in ferroelectric $Pb(ZrTi)O_3$ nanoparticles. *Phys. Rev. Lett.* **98**, 077603 (2007).
50. Z. Wu, N. Huang, Z. Liu, J. Wu, W. Duan, and B.-L. Gu: Unusual vortex structure in ultrathin $Pb(Zr_{0.5}Ti_{0.5})O_3$ films. *J. Appl. Phys.* **101**, 014112 (2007).
51. B.J. Rodriguez, X.S. Gao, L.F. Liu, W. Lee, I.I. Naumov, A.M. Bratkovsky, D. Hesse, and M. Alexe: Vortex polarization states in nanoscale ferroelectric arrays. *Nano Lett.* **9**, 1127 (2009).
52. J. Li, J.-F. Li, Q. Yu, Q.N. Chen, and S. Xie: Strain-based scanning probe microscopies for functional materials, biological structures, and electrochemical systems. *J. Materiomics* **1**, 3 (2015).
53. C.T. Nelson, B. Winchester, Y. Zhang, S.J. Kim, A. Melville, C. Adamo, C. M. Folkman, S.H. Baek, C.B. Eom, D.G. Schlom, L.Q. Chen, and X.Q. Pan: Spontaneous vortex nanodomain arrays at ferroelectric heterointerfaces. *Nano Lett.* **11**, 828 (2011).
54. C.L. Jia, K.W. Urban, M. Alexe, D. Hesse, and I. Vrejoiu: Direct observation of continuous electric dipole rotation in flux-closure domains in ferroelectric $Pb(Zr,Ti)O_3$. *Science* **331**, 1420 (2011).
55. L.J. McGilly, A. Schilling, and J.M. Gregg: Domain bundle boundaries in single crystal $BaTiO_3$ lamellae: searching for naturally forming dipole flux-closure/quadrupole chains. *Nano Lett.* **10**, 4200 (2010).
56. R.G.P. McQuaid, L.J. McGilly, P. Sharma, A. Gruverman, and J.M. Gregg: Mesoscale flux-closure domain formation in single-crystal $BaTiO_3$. *Nat. Commun.* **2**, 404 (2011).
57. Y.L. Tang, Y.L. Zhu, X.L. Ma, A.Y. Borisevich, A.N. Morozovska, E.A. Eliseev, W.Y. Wang, Y.J. Wang, Y.B. Xu, Z.D. Zhang, and S.J. Pennycook: Observation of a periodic array of flux-closure quadrants in strained ferroelectric $PbTiO_3$ films. *Science* **348**, 547 (2015).
58. Y.-H. Chu, L.W. Martin, M.B. Holcomb, and R. Ramesh: Controlling magnetism with multiferroics. *Mater. Today* **10**, 16 (2007).
59. C.A.F. Vaz: Electric field control of magnetism in multiferroic heterostructures. *J. Phys—Condens. Mater.* **24**, 33 (2012).
60. J.J. Wang, J.M. Hu, J. Ma, J.X. Zhang, L.Q. Chen, and C.W. Nan: Full 180 degrees magnetization reversal with electric fields. *Sci. Rep.* **6**, 07507 (2016).
61. T. Zhao, A. Scholl, F. Zavaliche, K. Lee, M. Barry, A. Doran, M.P. Cruz, Y. H. Chu, C. Ederer, N.A. Spaldin, R.R. Das, D.M. Kim, S.H. Baek, C.B. Eom, and R. Ramesh: Electrical control of antiferromagnetic domains in multiferroic $BiFeO_3$ films at room temperature. *Nat. Mater.* **5**, 823 (2006).
62. Y.H. Chu, L.W. Martin, M.B. Holcomb, M. Gajek, H. Shu Jen, H. Qing, N. Balke, Y. Chan Ho, D. Lee, H. Wei, Z. Qian, Y. Pei Ung, A. F. Rodriguez, A. Scholl, S.X. Wang, and R. Ramesh: Electric-field control of local ferromagnetism using a magnetoelectric multiferroic. *Nat. Mater.* **7**, 478 (2008).
63. J.T. Heron, M. Trassin, K. Ashraf, M. Gajek, Q. He, S.Y. Yang, D. E. Nikonov, Y.H. Chu, S. Salahuddin, and R. Ramesh: Electric-field-induced magnetization reversal in a ferromagnet-multiferroic heterostructure. *Phys. Rev. Lett.* **107**, 217202 (2011).
64. S.M. Wu, S.A. Cybart, P. Yu, M.D. Rossell, J.X. Zhang, R. Ramesh, and R. C. Dynes: Reversible electric control of exchange bias in a multiferroic field-effect device. *Nat. Mater.* **9**, 756 (2010).
65. S.M. Wu, S.A. Cybart, D. Yi, J.M. Parker, R. Ramesh, and R.C. Dynes: Full electric control of exchange bias. *Phys. Rev. Lett.* **110**, 067202 (2013).
66. L.W. Martin, Y.-H. Chu, Q. Zhan, R. Ramesh, S.-J. Han, S.X. Wang, M. Warusawithana, and D.G. Schlom: Room temperature exchange bias and spin valves based on $BiFeO_3/SrRuO_3/SrTiO_3$/Si (001) heterostructures. *Appl. Phys. Lett.* **91**, 172513 (2007).
67. L.W. Martin, Y.-H. Chu, M.B. Holcomb, M. Huijben, P. Yu, S.-J. Han, D. Lee, S.X. Wang, and R. Ramesh: Nanoscale control of exchange bias with $BiFeO_3$ thin films. *Nano Lett.* **8**, 2050 (2008).
68. J. Allibe, S. Fusil, K. Bouzehouane, C. Daumont, D. Sando, E. Jacquet, C. Deranlot, M. Bibes, and A. Barthélémy: Room temperature electrical manipulation of giant magnetoresistance in spin valves exchange-biased with $BiFeO_3$. *Nano Lett.* **12**, 1141 (2012).
69. H. Bea, M. Bibes, F. Ott, B. Dupe, X.H. Zhu, S. Petit, S. Fusil, C. Deranlot, K. Bouzehouane, and A. Barthelemy: Mechanisms of exchange bias with multiferroic $BiFeO_3$ epitaxial thin films. *Phys. Rev. Lett.* **100**, 017204 (2008).
70. F. Liu, Y. Zhou, Y.J. Wang, X.Y. Liu, J. Wang, and H. Guo: Negative capacitance transistors with monolayer black phosphorus. *NPJ Quantum Mater.* **1**, 16004 (2016).

https://doi.org/10.1557/mrc.2016.39 Published online by Cambridge University Press